Supporting information

Designer Ligand Field for Blue-green Luminescence of Organoeuropium(II) Sandwich Complexes with Cyclononatetraenyl Ligands

Kenshiro Kawasaki,[†] Rion Sugiyama, [†]Takashi Tsuji,[†,‡] Takeshi Iwasa, [†,‡] Hironori Tsunoyama,[†,‡] Yoshiyuki Mizuhata,[§] Norihiro Tokitoh,[§] Atsushi Nakajima*[,†,‡,//]

[†] Department of Chemistry, Faculty of Science and Technology, Keio University, 3-14-1 Hiyoshi, Kohoku-ku, Yokohama 223-8522, Japan.

[‡] Nakajima Designer Nanocluster Assembly Project, Exploratory Research for Advanced Technology (ERATO), Japan Science and Technology Agency, 3-2-1 Sakado, Kawasaki 213-0012, Japan.

[§] Institute for Chemical Research, Kyoto University, Gokasho, Uji, Kyoto 611-0011, Japan.

[//] Keio Institute of Pure and Applied Sciences (KiPAS), Keio University, 3-14-1 Hiyoshi, Kohoku-ku, Yokohama 223-8522, Japan.

General procedure

All the reactions were performed under an argon atmosphere using Schlenk line or glovebox techniques in dehydrated, deaerated solvents. Tetrahydrofuran (THF) and toluene were dried and deoxygenated on a solvent purification system (GlassContour, Nikko Hansen Co. Ltd.). Hexane (Wako Pure Chemical Industries, Ltd., deoxidized) and europium (II) iodide (EuI_2, Sigma-Aldrich, 99.9%) were used as received. Cyclooctatetraene (Cot, Sigma-Aldrich, 98%) and dichloromethyl methyl ether (Sigma-Aldrich, 98%) were deaerated with freeze-pump-thaw degassing before use. Potassium (K, Sigma-Aldrich, 98%) was used cut freshly in the glovebox. For NMR solvents, deuterated tetrahydrofuran (Kanto Chemical Co., Inc.) was dried over NaK, and vacuum-transferred before use. Deuterated chloroform (Kanto Chemical Co., Inc.) was used as received.

^{1}H NMR (399.65 MHz) was recorded on a JEOL JNM-AL400 spectrometer at room temperature (RT). In combustion analyses for C and H, all elemental analyses were performed in the Microanalytical Laboratory of the Institute for Chemical Research, Kyoto University. Laser desorption ionization time-of-fright mass spectrometry (LDI-TOF-MS) was performed on a Voyger DE-STR (ABSciex) mass spectrometer, where the sample was transferred under vacuum.

Synthesis of K(Cnt)

The synthesis of K(Cnt) was based on the procedure reported by Katz *et al*.[1] 9-methoxy bicyclo-[6.1.0]-nonatriene (300 mg, 2.02 mmol) was added to the mixture of potassium (406 mg, 10.38 mmol) and THF (1.2 mL) at –196°C. After heating to RT, the mixture was kept to stir for 24 h. Precipitation was removed by centrifugation in THF. After removal of THF from the supernatant under vacuum, the residue was washed with toluene to obtain K(Cnt) as ivory powder (231 mg, 1.48 mmol, 73%). 9-methoxy bicyclo-[6.1.0]-nonatriene ^{1}H NMR ($CDCl_3$, 298 K): δ 6.01 (m, 6H), 3.44 (s, 3H), 2.73 (t, 1H), 1.68 (d, 2H), K(Cnt) ^{1}H NMR (C_4D_8O, 298 K): δ 7.04 (s, 9H), ^{13}C NMR (C_4D_8O, 298 K): δ 111.0 (s, 9C).

Synthesis of 1-Eu

1-Eu was synthesized based on a reported procedure for $(Cnt)_2Ba$ [2] with slight modifications (Scheme 1). A THF suspension (6 mL) of EuI_2 (498 mg, 1.23 mmol) was added to a THF solution (4 mL) of K(Cnt) (386.2 mg, 2.47 mmol) at RT. The solution gradually became pale yellow and yellow powder including KI was gradually precipitated. After 24 h, the mixture was centrifuged to remove the yellow precipitation and solvents were removed from supernatant. A pale yellow powder of supernatant was then extracted with toluene. After centrifugation to remove immiscible byproducts and evaporation of toluene, dried crude products were suspended in hexane. The products insoluble in hexane were precipitated by centrifugation and dried under vacuum, and finally an orange powder of **1-Eu** (19.6

mg, 4%) was obtained. Crystals suitable for X-ray analysis were obtained by slow concentration from a saturated toluene solution at RT. Elemental analysis; calcd. for $(C_9H_9)_2Eu$: C, 55.97; H, 4.70; Eu, 39.3. Found: C, 57.21; H, 5.18; Eu, 38.5. MALDI-MS; calcd. for $[(Cnt)_2Eu]$: 387.1. Found: 389.6 $[(Cnt)_2Eu]^-$.

General procedure for characterization of 1-Eu

Concentration of Eu in **1-Eu** was determined by inductively coupled plasma atomic emission spectroscopy (ICP-AES) (SPS1700HVR, Seiko Instruments). Powder of **1-Eu** was weighted into a round bottom flask in the glovebox. Following oxidation of the specimen by slow exposure to air, a mixed solution of sulfuric and nitric acid (4 mL : 16 mL) was added to the sample. The mixed solution was heated at 120°C until all the **1-Eu** was dissolved. The dissolved specimen was diluted to 100 mL with ultrapure water. The Eu concentration was quantified against external standards based on emission lines of emitting at 281.394 nm.

The infrared (IR) absorption spectra of **1-Eu** were measured by the KBr method using an FT-IR spectrometer (ALPHA, Bruker). Sample pellets were sealed in a homemade stainless steel cell with two NaCl windows under an argon atmosphere. Raman spectra were recorded using a Raman spectrometer (inVia Raman Microscope, Renishaw) with excitation of a He−Ne laser (632.8 nm), where the sample was sealed in a quartz capillary under an argon atmosphere.

The magnetic susceptibilities of **1-Eu** were determined by a SQUID magnetometer (MPMS XL, Quantum Design) from 2 to 224 K in an applied field of 4000 Oe. Samples were encapsulated in borosilicate glass tubes under vacuum.

Optical absorption in the ultraviolet–visible region was measured by a spectrophotometer (V-670, JASCO). Photoluminescence (PL) spectra were measured by a spectrofluorometer (Fluorolog-3, Horiba JobinYvon). For these measurements at RT, the powder samples were dissolved in toluene and sealed in a septum-capped quartz cell under argon. For measurements at 77 K (liquid nitrogen), toluene solution of **1-Eu** sealed in a quartz tubing was placed in a dewar filled with liquid nitrogen. Absorbance was scaled by a Jacobian factor ($dE/d\lambda$), where E is the photon energy and λ the wavelength of the light, in order to conserve the integrated spectral area through the conversion of spectra from wavelength domain to energy domain. The resulting relationship between Abs(E) and Abs(λ) was $Abs(E)=Abs(\lambda)/(dE/d\lambda)\propto Abs(\lambda)\times\lambda^2$. The fluorescence quantum yields (Φ_f) of **1-Eu** in toluene was determined by comparing its integrated emission intensities with those of coumarin153 ($\Phi_f = 0.546$ in ethanol).[3]

SC-XRD data collection and refinements

Single crystal of **1-Eu** was obtained from its toluene solution. The crystals were mounted in a Fomblin® Y oil on a glass fiber. Low-temperature (103 K) data were collected on a RIGAKU Saturn70 CCD system with VariMax Mo Optic using Mo Kα radiation (λ = 0.71075 Å) with φ- and ω-scans. An empirical absorption correction was applied to the diffraction data using MULABS.[4] The structure were solved by direct methods using SHELXS and refined against F^2 on all data by full-matrix least squares with SHELXL.[5] All non-hydrogen atoms were refined anisotropically. All hydrogen atoms were refined using a riding model. The isotropic displacement parameters of all hydrogen atoms were fixed to 1.2 times the U_{eq} value of the atoms they are linked to. Descriptions of the individual refinements follow below and details of the data quality and a summary of the residual values of the refinements for all structures are given in Table S1.

Complex **1-Eu** crystallized in the monoclinic space group $P2_1/n$ with 0.5 molecule per asymmetric unit. The model contains no solvent. No counter anions or cations are found in the SC-XRD analysis. As for the Cnt ring, the slipped disorder (C10-C18) was observed. The major/minor ratio was 0.58:0.42. RIGU functions were used for the atoms on the Cnt rings.

Details of computations

All the calculations for $(Cnt)_2Eu$ and $[Li(Cot)_2]_2Eu$ were performed by TURBOMOLE 6.4-6.5 [6] at the RI-B3LYP level[7,8] using the def-SV(P) basis sets[9] along with the 28-electron relativistic effective core potential for Eu [10]. Raman spectra were computed from the static polarizability gradient, obtained by the EGRAD module [11,12] implemented in the TURBOMOLE program package. The electronic

absorption spectra were simulated by TD-DFT [13-16], wherein the line spectra are convolved by a Lorentzian with full width at half-maximum (FWHM) = 0.01 eV. Molecular orbitals and electrostatic potentials are visualized by TmoleX and VESTA [17], respectively.

Table S1. Experimental crystal data for the X-ray diffraction of **1-Eu**.

Empirical formula	$C_{18}H_{18}Eu$
Formula weight	386.28
Temperature	103(2) K
Wavelength	0.71075 Å
Crystal system	Monoclinic
Space group	$P2_1/n$ (#14)
Unit cell dimensions	a = 7.2625(2) Å α = 90°.
	b = 9.0561(4) Å β = 99.710(3)°.
	c = 11.2528(7) Å γ = 90°.
Volume	729.49(6) Å^3
Z	2
Density (calculated)	1.759 Mg/m^3
Absorption coefficient	4.282 mm^{-1}
F(000)	378
Crystal size	0.20 x 0.10 x 0.05 mm^3
θ range for data collection	2.904 to 27.750°.
Index ranges	-9<=h<=9, -11<=k<=11, -14<=l<=14
Reflections collected	9040
Independent reflections	1712 [R(int) = 0.0336]
Completeness to θ = 25.242°	99.8 %
Refinement method	Full-matrix least-squares on F^2
Data / restraints / parameters	1712 / 108 / 170
Goodness-of-fit on F^2	1.137
Final R indices [I>2□(I)]	R_1 = 0.0186, wR_2 = 0.0374
R indices (all data)	R_1 = 0.0246, wR_2 = 0.0397
Extinction coefficient	n/a
Largest diff. peak and hole	0.472 and -0.675 e.Å^{-3}

Table S2. Bond lengths (Å) and bond angles (deg.) for **1-Eu**.

Eu(1)-C(1)	2.865(8)
Eu(1)-C(2)	2.889(9)
Eu(1)-C(3)	2.886(9)
Eu(1)-C(4)	2.882(8)
Eu(1)-C(5)	2.888(7)
Eu(1)-C(6)	2.929(7)
Eu(1)-C(7)	2.958(6)
Eu(1)-C(8)	2.923(7)
Eu(1)-C(9)	2.878(6)

Eu(1)-C(10)	2.903(11)
Eu(1)-C(11)	2.862(13)
Eu(1)-C(12)	2.832(13)
Eu(1)-C(13)	2.796(13)
Eu(1)-C(14)	2.798(11)
Eu(1)-C(15)	2.812(9)
Eu(1)-C(16)	2.823(9)
Eu(1)-C(17)	2.860(7)
Eu(1)-C(18)	2.882(8)
C(1)-C(9)	1.395(12)
C(1)-C(2)	1.399(11)
C(2)-C(3)	1.405(10)
C(3)-C(4)	1.390(9)
C(4)-C(5)	1.385(8)
C(5)-C(6)	1.371(8)
C(6)-C(7)	1.398(9)
C(7)-C(8)	1.401(11)
C(8)-C(9)	1.390(12)
C(10)-C(18)	1.414(11)
C(10)-C(11)	1.448(13)
C(11)-C(12)	1.365(14)
C(12)-C(13)	1.353(15)
C(13)-C(14)	1.374(17)
C(14)-C(15)	1.365(15)
C(15)-C(16)	1.413(14)
C(16)-C(17)	1.394(13)
C(17)-C(18)	1.396(11)

C(9)-C(1)-C(2)	140.3(8)
C(1)-C(2)-C(3)	139.5(8)
C(4)-C(3)-C(2)	139.5(8)
C(5)-C(4)-C(3)	139.7(8)
C(6)-C(5)-C(4)	141.5(8)
C(5)-C(6)-C(7)	140.3(7)
C(6)-C(7)-C(8)	138.8(6)
C(9)-C(8)-C(7)	140.1(6)
C(8)-C(9)-C(1)	140.1(7)
C(18)-C(10)-C(11)	138.3(10)
C(12)-C(11)-C(10)	142.9(12)
C(13)-C(12)-C(11)	140.0(12)
C(12)-C(13)-C(14)	138.7(11)
C(15)-C(14)-C(13)	140.7(10)
C(14)-C(15)-C(16)	141.1(9)
C(17)-C(16)-C(15)	140.5(9)
C(16)-C(17)-C(18)	139.7(9)
C(17)-C(18)-C(10)	137.6(10)

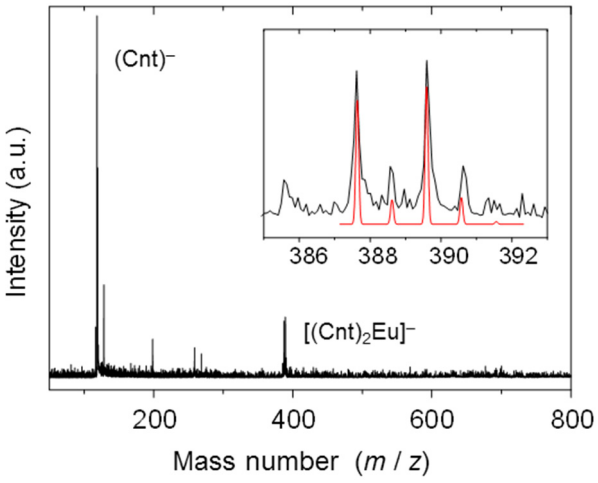

Figure S1. Negative ion laser-desorption ionization mass spectrum of **1-Eu**. Isotope pattern of $(Cnt)_2Eu$ was also shown in red.

Table S3. Comparison of representative bond lengths (Å) and tilting angles (deg.) of sandwich complexes of divalent europium.

	1-Eu	**$[(Cp^*)Eu]_2(Cot)$[a]**	**$[(THF)_3K(Cot)]_2Eu$[b]**	**$((i\text{-}Pr)_4C_4H)_2Eu$[c]**	**$(Cp^{BIG})_2Eu$[d]**	**$(C_5Ph_5)_2Eu$[e]**
			Bond length (Å)			
Eu–C (Cp ring)	–	2.77, 2.81	–	2.8077 – 2.8448	2.772 – 2.782	2.751 – 2.788
Eu–C (Cot or Cnt)	2.801 – 2.853	2.81, 2.83	2.780 – 2.809	–	–	–
Eu–cntr.[f] (Cp)	–	2.506, 2.532	–	2.504 – 2.510	2.497	2.489
Eu–cntr.[f] (Cot or Cnt)	2.068 2.024	2.129, 2.166	2.153	–	–	–
			Tilting angle (deg.)			
Cntr.[f] –Eu–cntr.	180.00	147.2, 149.5	180.0	168.1, 165.5	180	180

a) Evans, W. J.; Johnston, M. A.; Greci, M. A.; Ziller, J. W., Synthesis, Structure, and Reactivity of Unsolvated Triple-Decked Bent Metallocenes of Divalent Europium and Ytterbium. *Organomet*. **1999**, 18, 1460-1464.

b) Evans, W. J.; Shreeve, J. L.; Ziller, J. W., Synthesis and Structure of inverse cyclooctatetraenyl Sandwich Complexes of Europium(II): $[(C_5Me_5)(THF)_2Eu]_2(\mu\text{-}C_8H_8)$ and $[(THF)_3K(\mu\text{-}C_8H_8)]_2Eu$. *Polyhedron* **1995**, 14, 2945.

c) Sitzmann, H.; Dezember, T.; Schmitt, O.; Weber, F.; Wolmershäuser, G.; Ruck, M., Metallocenes of Samarium, Europium, and Ytterbium with the Especially Bulky Cyclopentadienyl Ligands $C_5H(CHMe_2)_4$, $C_5H_2(CMe_3)_3$, and $C_5(CHMe_2)_5$. *Z. Anorg. Allg. Chem.* **2000**, 626, 2241-2244.

d) Harder, S.; Naglav, D.; Ruspic, C.; Wickleder, C.; Adlung, M.; Hermes, W.; Eul, M.; Pöttgen, R.; Rego, D. B.; Poineau, F.; Czerwinski, K. R.; Herber, R. H.; Nowik, I., Physical Properties of Superbulky Lanthanide Metallocenes: Synthesis and Extraordinary Luminescence of $[EuII(CpBIG)_2]$ (CpBIG=(4-$nBu\text{-}C_6H_4)_5$-Cyclopentadienyl). *Chem. Eur. J.* **2013**, 19, 12272-12280.

e) Kelly, R. P.; Bell, T. D. M.; Cox, R. P.; Daniels, D. P.; Deacon, G. B.; Jaroschik, F.; Junk, P. C.; Le Goff, X. F.; Lemercier, G.; Martinez, A.; Wang, J.; Werner, D., Divalent Tetra- and Penta-phenylcyclopentadienyl Europium and Samarium Sandwich and Half-Sandwich Complexes: Synthesis, Characterization, and Remarkable Luminescence Properties. *Organomet.* **2015**, 34, 5624-5636.

f) Cntr. = centroid

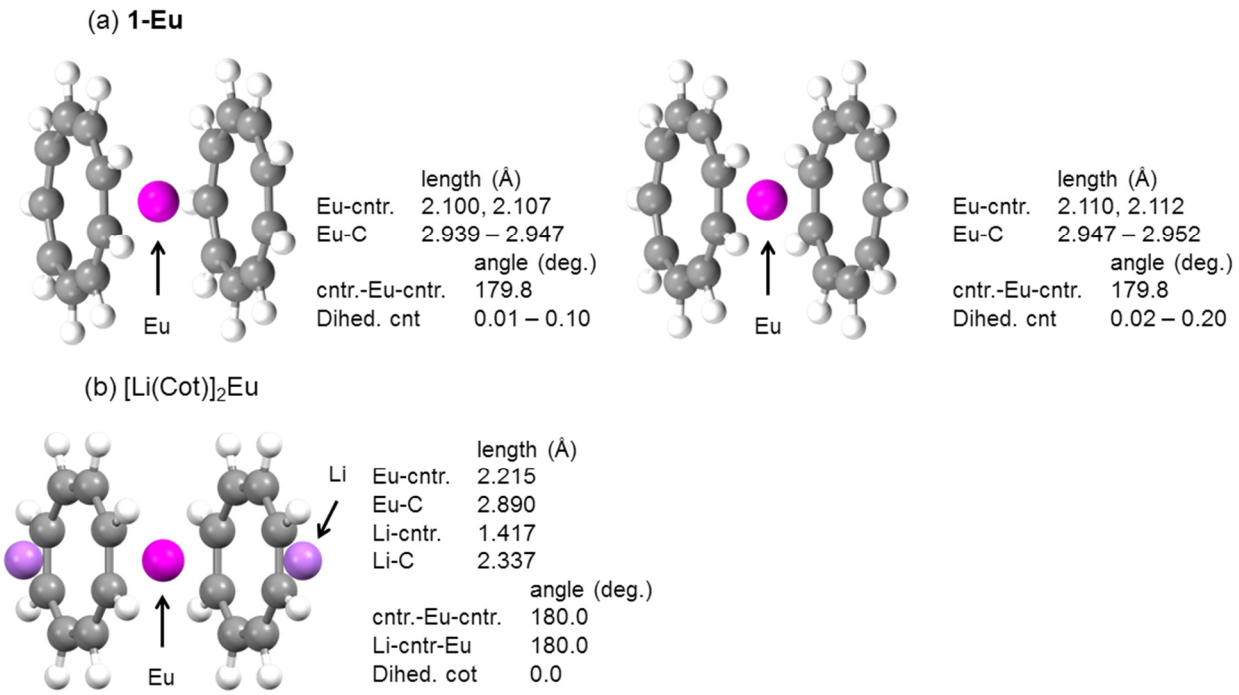

Figure S2. Optimized structure of (a) **1-Eu** and (b) $[Li(Cot)]_2Eu$ calculated at B3LYP/def-SV(P) level. Total energies of two isomers of **1-Eu** were almost the same (ΔE=1 meV). The energy of Kohn-Sham orbitals and electron excitation were also consistent for these isomers. Pseudo D_9 isomer was used for TD-DFT and vibrational analysis. Potential barrier for rotation of Cnt ring (transformation between two isomers of 1-Eu) is less than 10 meV.

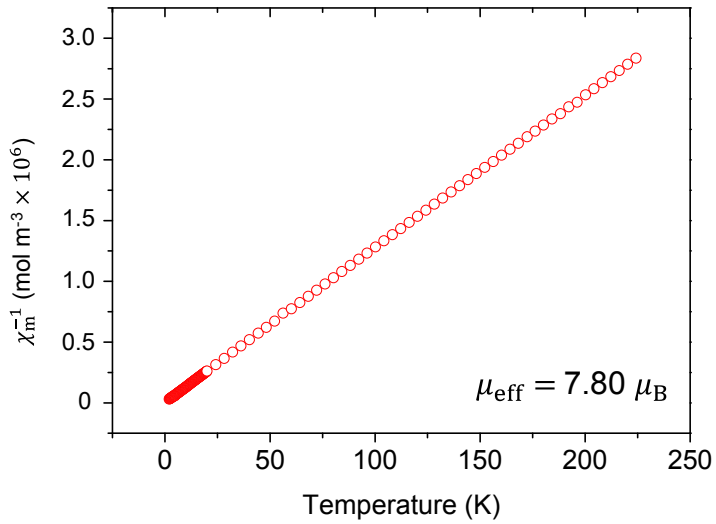

Figure S3. Inverse magnetic susceptibility plots of χ_m^{-1} at 4000 Oe from 2 to 224 K. The effective magnetic moment of **1-Eu** was evaluated as 7.80 μ_B from the gradient of linear fit for the data at 2-224 K.

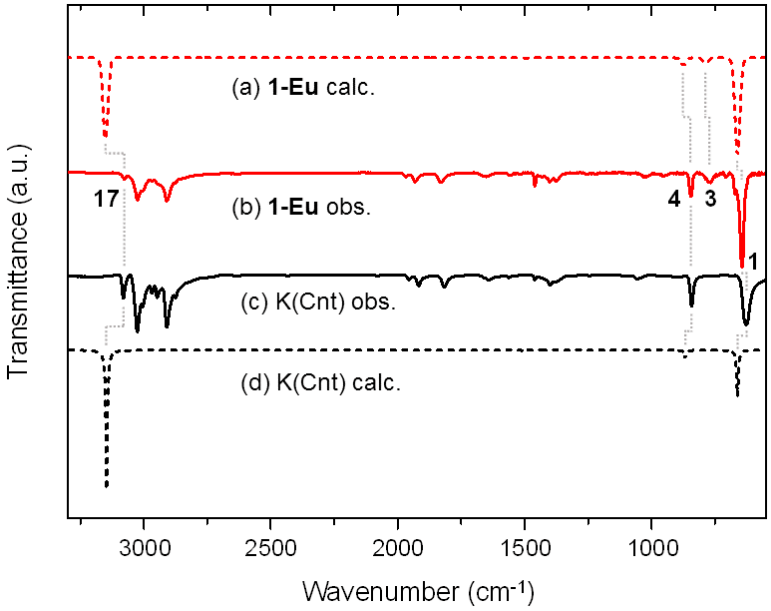

Figure S4. Experimental (solid lines) and calculated IR spectra (dotted lines) of **1-Eu**. (a) **1-Eu** calc., (b) **1-Eu** obs. (c) K(Cnt) obs., and (d) K(Cnt) calc. Calculations were performed at B3LYP/def-SV(P) level.

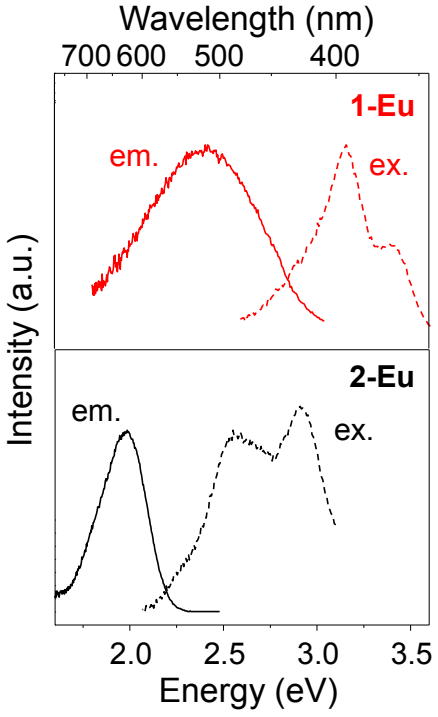

Figure S5. PL excitation (dotted lines) and emission (solid lines) spectra of **1-Eu** and **2-Eu** in toluene at RT. For **1-Eu**, λ_{em} = 516 nm, λ_{ex} = 390 nm. For **2-Eu**, λ_{em} = 630 nm, λ_{ex} = 485 nm. At RT, the emission bands for both complexes are significantly broadened (FWHM = 0.11 eV to 0.73 eV for **1-Eu** and 0.13 eV to 0.30 eV for **2-Eu**). The Stokes shift at RT (0.77 eV) becomes larger for **1-Eu**, which is due to the absence of the first excitation maximum. Stokes shift for **2-Eu** at RT (0.57 eV) is almost the same as that at 77 K.

Table S4. Assignments of Raman spectra of **1-Eu** based on theoretical calculation (B3LYP/def-SV(P)) level.

1-Eu obs. (cm^{-1})	**1-Eu** calc. (cm^{-1})	Assignment
140	114	Ring-metal str.
178	123, 112	ring-metal titl.
295	277, 282	in-plane CCC bend.
677	694	ring breath.
1517	1560	in-plane CH bend..
	3136, 3150	CH str.

Table S5. Assignments of IR spectra of **1-Eu** based on theoretical calculation (B3LYP/def-SV(P) level.

	K(Cnt) obs. (cm^{-1})	K(Cnt) calc. (cm^{-1})	**1-Eu** obs. (cm^{-1})	**1-Eu** calc. (cm^{-1})	Assignment
1	625	661	642	662	out-of-plane CH bend.
2			708		
3			770	786	out-of-plane CH bend.
4	844	867	844	872	in-plane CH bend.
5			949		
6	1055		1027		
7	1375		1373		
8	1399		1400		
9	1459	1514	1459	1490	in-plane CH bend.
10	1562		1555		
11	1640		1651		
12	1817		1830		
13	1917		1931		
14	1956		1969		
15	2910		2910		
16	3025		3024		
17	3082	3146	3077	3152	CH str.

Table S6. Comparison of frequencies for stretching and tilting modes between Eu ion and ligands in sandwich complexes.

	$[(DME)Li(Cot'')]_2Eu$[a]		$[(DME)Li(Cot)]_2Eu$[a]		**1-Eu**		Eu-Cot(1:1)[b]	
	Exp.	Calc.	Exp.	Calc.	Exp.	Calc.	Exp.	Calc.
Str.	131	109	97	129	140	111	191	N/D
Tilt.	131	109	97	133	178	139	211	N/D

a) T. Tsuji *et al., Chem. Phys. Lett.,* **2014**, 595-596, 144-150., b) T. Tsuji *et al., J. Phys. Chem. C*, **2014**, 118, 5896-5907

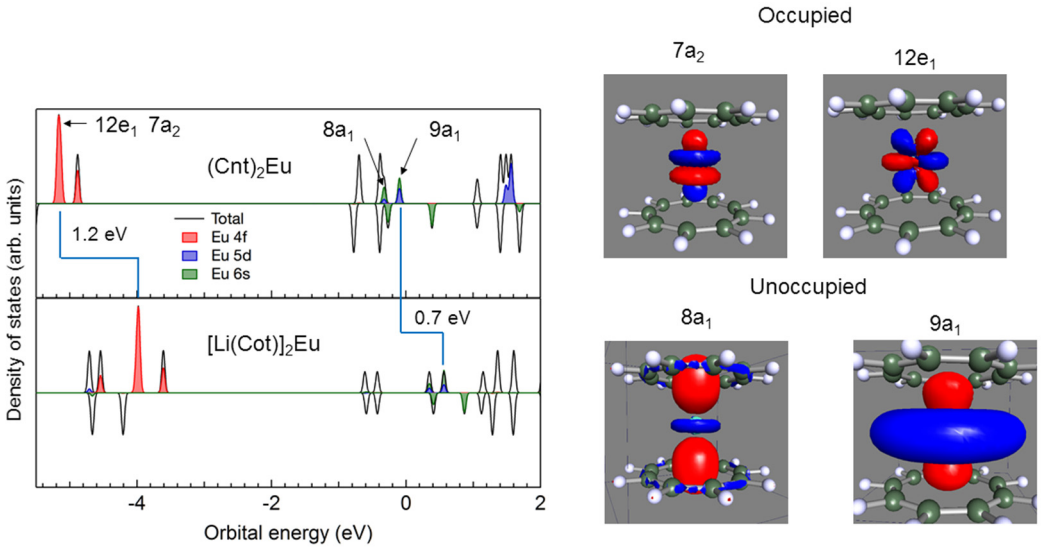

	Excitation energy		Assignments of electronic transition			
	Wavelength (nm)	Energy (eV)	orbitals	contribu-tion	orbitals	contribu-tion
1st	426	2.91	$12e_1$ to $9a_1$	70.3%	$12e_1$ to $8a_1$	26.2%
2nd	422	2.93	$7a_2$ to $9a_1$	70.1%	$7a_2$ to $8a_1$	26.1%

Figure S6. (left) Comparison of density-of-states for **1-Eu**, $[Li(Cot)]_2Eu$. (right) Isosurfaces (0.03 e/a.u.^{3}) for molecular orbitals of **1-Eu** relating to the first and second electronic transitions calculated by TD-DFT (B3LYP/def-SV(P)).

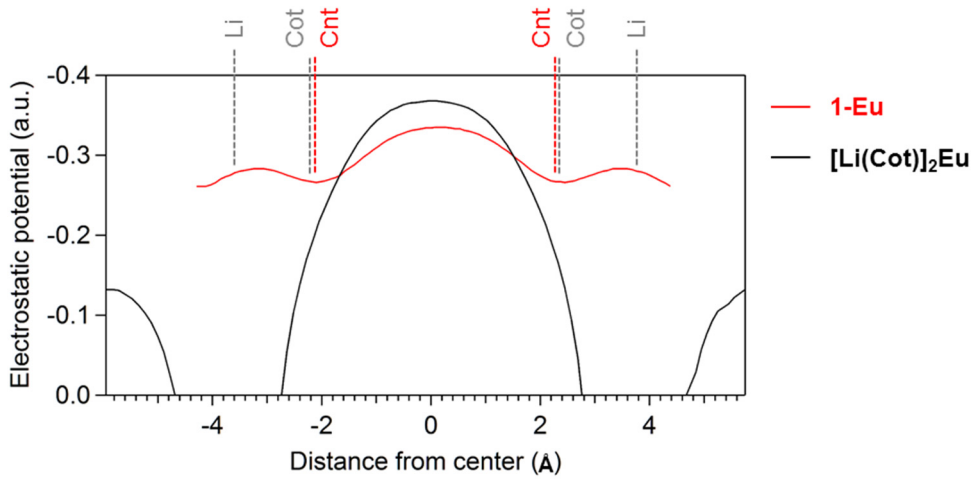

Figure S7. Electrostatic potential curve along the molecular axis for $(Cnt)_2Eu$ (red) and $[Li(Cot)]_2Eu$ (black) calculated at B3LYP/def-SV(P) level.

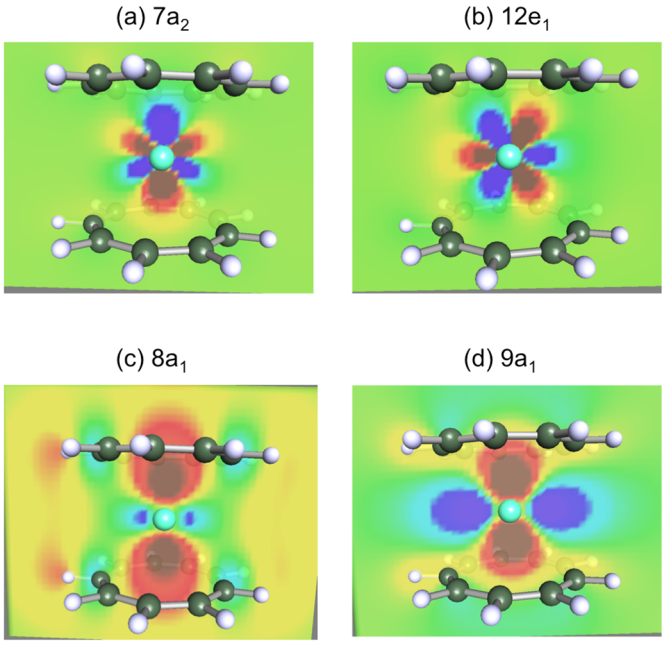

Figure S8. Molecular orbitals of $(Cnt)_2Eu$. The occupied orbitals (Eu 4f) of (a) $7a_1$, (b) $12e_1$, and unoccupied orbitals (Eu 6s-$5d_{z2}$) of (c) $8a_1$, (d) $9a_1$ calculated at B3LYP/def-SV(P) level. Contour maps of electron density are shown in R-G-B scale (Red: positive, blue: negative phase of wavefunctions)

References

[1] Katz, T. J. et al., *J. Am. Chem. Soc.,* 1964, **86**, 5194.

[2] Walter, M. D. et al., *J. Am. Chem. Soc.,* 2005, **127**, 17494.

[3] Rurack, K.; Spieles, M., *Anal. Chem.,* 2011, **83**, 1232-1242.

[4] Blessing, R. H., *Acta. Crystallogr. Sect. A,* 1995, **A51**, 33.

[5] Sheldrick, G. M., *Acta Crystallogr. Sect. A,* 2008, **A64**, 112.

[6] TURBOMOLE V6.2 2010 – V6.4 2012, A development of University of Karlsruhe and Forschungszentrum Karlsruhe GmbH, 1989-2007, TURBOMOLE GmbH, since 2007; available from http://www.turbomole.com.

[7] Lee, C.; Yang, W.; Parr, R.G.; *Phys. Rev. B,* 1988, **37**, 785.

[8] Becke, A.D., *J. Chem. Phys.,* 1993, **98**, 5648.

[9] Schäfer, A.; Horn, H.; Ahlrichs, R., *J. Chem. Phys.,* 1992, **97**, 2571.

[10] Eichkorn, K.; Weigend, F.; Treutler, O.; Ahlrichs, R.; *Theor. Chem. Acc.,* 1997, **97**, 119.

[11] Furche, F.; Ahlrichs, R., *J. Chem. Phys.,* 2002, **117**, 7433.

[12] Rappoport, D.; Furche, F., *J. Chem. Phys.,* 2007, **126**, 201104.

[13] Casida, M. E., *Recent Advances in Density Functional Methods Part I*; D.P. Chong, (Ed.); World Scientific, Singapore, 1995, p. 155.

[14] Bauernschmitt, R.; Ahlrichs, R., *Chem. Phys. Lett.,* 1996, **256**, 454.

[15] Bauernschmitt, R.; Häser, M.; Treutler, O.; Ahlrichs, R., *Chem. Phys. Lett.,* 1997, **264**, 573.

[16] Furche, F., *J. Chem. Phys.,* 2001, **114**, 5982.

[17] Momma, K.; Izumi, F.; *J. Appl. Crystallogr.,* 2011, **44**, 1272.